JOURNAL OF MATERIALS SCIENCE: MATERIALS IN MEDICINE 6 (1995) 311–318

Apatite-mullite glass-ceramics

R. HILL
Department of Materials Science and Technology, University of Limerick, Limerick, Ireland
D. WOOD
Leeds Dental Institute, University of Leeds, Leeds LS2 9JT, UK

Two series of fluoro-alumino-silicate glasses, one with varying phosphate content (P_2O_5) and one with fixed phosphate content and varying fluorite (CaF_2) content have been investigated as potential bioglass-ceramics. Compositions with intermediate phosphate contents that contained fluorite crystallized to fluoroapatite and mullite. Compositions with high fluorite contents exhibited a low liquidus temperature, were readily castable and crystallized by a bulk nucleation mechanism. The fluoroapatite phase with appropriate heat treatment formed as thin needle-like crystals with a high aspect ratio.

1. Introduction

Many glass-ceramics have been developed for both bone substitutes and dental crowns during the last 20 years. Glass-ceramic bone substitutes are largely based on glasses that crystallize to an apatite phase [1–5]. They generally fall into two distinct groups, the apatite–wollastonite, A–W, ceramics developed by Kokubo *et al.* [1] and the mica-based materials originally developed by Beall *et al.* [2] and Grossman [3] for dental crowns.

In the A–W ceramics, it is the needle-shaped wollastonite crystallites that impart high strength and fracture toughness to the final glass-ceramic [6]. In the Bioverit material, it is a mica-type phase that imparts machinability and strength. The mica-type materials generally contain a significant alkali metal ion content, which results in *in vivo* degradation of mechanical properties. Furthermore, the strength and machinability of these materials is always comprised at the expense of obtaining sufficient bioactivity. The A–W ceramics based on SiO_2–P_2O_5–CaO–MgO are probably the most promising bone substitute materials, however, the processing route for these materials is not the classic glass-ceramic route of converting a monolithic glass to a monolithic ceramic, but involves sintering a glass-ceramic powder. Thus all the processing advantages of being able to cast as a glass prior to converting through to a ceramic are lost.

The sintering production route for these materials is a major disadvantage and would make it relatively expensive and difficult to produce the complex shapes required of prostheses. The classic glass-ceramic production route is not possible for the A–W ceramics, since wollastonite undergoes surface nucleation, rather than bulk nucleation.

Over 20 years ago [7] the advantages of producing teeth for dentures by a glass-ceramic route was recognized. The glass casting route eliminated defects introduced during a slurry process for porcelain teeth production and teeth could be cast to shape without significant shrinkage. Clearly, glass-ceramics offer considerable potential for producing dental crowns. At least three types of glass-ceramic crown materials are available, commercially these include materials based on the Li_2O–ZnO–SiO_2 system, the SiO_2–P_2O_5–CaO–MgO system and a material based on fluormica crystallites.

The first two systems are designed to be castable i.e. the crown is cast in the glassy state and then converted to a ceramic by appropriate heat treatment. The Li_2O–ZnO–SiO_2 system exhibits a relatively low liquidus and is consequently very easy to cast. In contrast, the "Ceraspear" crown based on the SiO_2–P_2O_5–CaO–MgO [8, 9] system is more difficult to cast, requiring a temperature of 1450 °C. However, this latter system crystallizes to an oxyapatite phase which converts to hydroxyapatite on the surface in the presence of moisture.

There are obvious advantages to having an apatite phase present, notably a similar hardness to enamel and biocompatibility, but also, apatite materials have the capacity to bond chemically with glass-ionomer cements and thus crowns based on apatite phases could be readily bonded in place without further treatment.

The Ceraspear material (like the A–W ceramics, which are also based on the SiO_2–P_2O_5–CaO–MgO system) is susceptible to surface crystal nucleation [10], which results in an unacceptable reduction in strength, since the large surface crystallites act as Griffith flaws, as well as resulting in a reduction in the aesthetic appearance of the crown.

The third glass-ceramic material commercially available is the Dicor crown [11] which is machinable using conventionally tipped tools and is based on fluormica crystallites. While the processing route of

0957–4530

direct machining to shape is attractive with this material, the material itself lacks strength. The high capital cost of the equipment needed to carry out the precision machining has resulted in most Dicor crowns being produced by a lost wax technique.

At this stage it is worth briefly outlining the ideal design criteria of a glass-ceramic bone substitute and castable dental crown.

An ideal glass-ceramic bone substitute and crown would:

(a) crystallize readily to an apatite phase;
(b) be readily castable into complex shapes at modest temperatures;
(c) undergo bulk crystal nucleation with no significant surface crystallization, resulting in a fine-grained material with high strength and fracture toughness;
(d) be bioactive, stimulating bone growth probably by the release of calcium, phosphate and especially fluoride ions. The fluoride ion is known to be smaller than the hydroxyl ion and as a consequence it fits better within the apatite lattice [14] and consequently fluoroapatite is thermally and chemically [15–18] more stable than hydroxyapatite. If the apatite phase in bone is considered to be in dynamic equilibrium with Ca^{2+} ions and PO_4^{3-} ions in solution as shown below:

$$Ca_5(PO_4)_3OH = 5Ca^{2+} + 3PO_4^{3-} + OH^-$$

any species that stabilises the apatite phase such as fluoride ions is going to strongly favour apatite deposition.

Similarly in the case of tooth enamel and dentine fluoroapatite is known to be far less soluble in acids than the closely related hydroxyapatite.

In the case of a dental crown, it is also important to be able to match the appearance of the crown to that of natural tooth. Thus crowns are required to be translucent and ideally would fluoresce in a similar fashion to natural teeth. Materials based on apatites are particularly desirable, since it is thought to be the apatite phase, doped with transition metals, that give rise to the luminescent character of teeth. To be able to obtain the required translucency, it is clearly necessary to be able to control the crystal nucleation process and the final crystallite size. In order for a castable dental crown to be commercially successful, it will almost certainly have to utilize the furnaces currently available in commercial dental laboratories for producing either the existing porcelain crowns or cobalt chrome prostheses. This places an upper limit for a castable crown of approximately 1300 °C. To be attractive to the dental technician a fast ceramming cycle is also required.

Marquis [10] has also stipulated a strength approaching 400 MPa with a high Weibull modulus for a crown suitable for posterior use without metal reinforcement.

During a recent study on ionomer glasses that form the basis of glass-ionomer cements used in dentistry, it was found that some commercial compositions crystallize readily to an apatite phase and mullite [12].

A previous study had also demonstrated that the problem of the loss of silicon tetrafluoride from these glasses could be overcome by incorporating a basic oxide. Thus it became practicable to develop a new range of apatite–mullite glass-ceramics. Such glass-ceramics are potentially attractive materials, since the high fluoride content of these glasses results in relatively low liquidus temperatures and low viscosity melts, which should in principle be castable at modest temperatures ($< 1300\,^{\circ}C$). Furthermore, apatite and mullite are desirable phases, since they both form needle-shaped crystals and there is thus potential for developing a microstructure based on interlocking needles with a high fracture toughness. Mullite is also a desirable phase, since it has a low coefficient of thermal expansion and is chemically inert under most conditions. The high fluoride content of these glasses is also attractive in that the final ceramic may well release fluoride ions in a similar fashion to glass-ionomer cements. Fluoride ions are known to stimulate bone growth [13], have an antimicrobial action and prevent secondary tooth decay by ion exchange with hydroxyl ions in hydroxyapatite.

F^- ion release is particularly desirable, since it is questionable whether the fluoride ion release from a thin layer of a glass-ionomer luting cement is sufficient to prevent secondary caries beneath existing crowns.

2. Experimental procedures

Two series of glasses were prepared based on the generic composition:

$$2\text{-}X SiO_2.XP_2O_5.Al_2O_3.CaO.YCaF_2$$

In the first series of glasses, Series A, Y was fixed at 1 and X varied from 0 to 1; there is thus a systematic substitution of one silicon ion by two phosphorous ions. Phosphorous pentoxide has a similar structural role to silica and acts as a network-forming oxide. In the second series of glasses, Series B, X was kept constant at 0.5 and Y was varied from 0 to 1. In this second series of glasses, both the calcium to phosphorous ratio and fluorine content of the glass is being altered. It is worth noting that there are sufficient calcium ions present in these glasses to enable all the aluminium atoms to take up a tetrahedral role within the glass network. Table I shows the composition of the A and B series glasses along with their respective firing temperatures and calcium-to-phosphates ratio. Both Series A and Series B glasses differ from existing commercial ionomer glasses in that they contain a basic oxide in the form of calcium oxide which helps eliminate fluorine loss from the melt [17].

Prior to studying the A and B series glasses a multicomponent glass with a similar composition to the ionomer glasses used commercially for dental cements was also prepared. The composition of this glass prior to melting is given in Table II.

All the A and B series glasses were prepared by melting appropriate amounts of silica (SiO_2), phosphorous pentoxide (P_2O_5), calcium carbonate

TABLE I Composition of A and B series glasses

Glass code	X	Y	Ca:P	Melt temperature (°C)
A1	O	1.0	–	1350
A2	0.250	1.0	4.00	1350
A3	0.375	1.0	2.66	1450
B1/A4	0.500	1.0	2.00	1380
A5	0.750	1.0	1.33	1380
A6	1.000	1.0	1.00	1350
B1/A4	0.5	1.0	2.00	1380
B2	0.5	0.75	1.75	1420
B3	0.5	0.50	1.50	1470
B4	0.5	0.25	1.25	1470
B5	0.5	0	1.00	1500

TABLE II Composition of commercial ionomer glass (weights in grams prior to firing)

Material	Weight (g)
SiO_2	175
Al_2O_3	100
CaF_2	90
Na_2AlF_6	135
AlF_3	32
$AlPO_4$	170

($CaCO_3$) and calcium fluoride (CaF_2) in lidded sillimanite crucibles at temperatures between 1300 and 1500° for 1.5 h. The resulting glass melts were then either shock quenched directly into water to produce frit, or cast into preheated graphite moulds to produce monolithic glass samples. The glass frits were ground and sieved to produce three particle size fractions < 45 μm, > 45 μm to < 125 μm and > 125 μm.

3. Glass characterization

The glass powders produced were characterized by X-ray powder diffraction using a Rigaku miniflex diffractometer (Rigaku Corporation, Tokyo, Japan.) interfaced to a microcomputer to permit step counting, and also by differential thermal analysis (DTA) using a Stanton Redcroft DTA 673-4 (Stanton Redcroft, Copper Mill Lane, Wimbledon, London, UK). A heating rate of 10 °C min^{-1} was used along with matched platinum/rhodium crucibles with alumina as the reference. Samples of glass powder (< 45 μm) and frit were heated at 10 °C min^{-1} to various temperatures in a tube furnace to simulate the DTA analysis in order to identify the various transitions occurring. The heat-treated powder was examined by X-ray powder diffraction and the pieces of frit were fractured and the fresh fracture surface etched in 5% hydrofluoric acid for 15 s, then examined by scanning electron microscopy using a Cambridge Instruments Stereoscan 90. Some selected samples of cast glasses, or heat-treated cast material were examined using a carbon replica technique after polishing and etching in an AEI EMA 802 (AEI, PO Box No. 1, Harlow, Essex, UK) transmission electron microscope.

4. Results and discussion

All the glasses produced in the form of frit were completely amorphous and devoid of any crystalline phases. The commercial-type glass composition exhibited two distinct glass transition temperatures in its DTA trace (Fig. 1) indicating that this glass has undergone amorphous phase separation (APS) despite being optically clear. Further evidence for this glass having undergone APS is provided by the acid leaching studies of Wasson and Nicholson [18]. Heat treatment to 930 °C for 20 min (well in excess of the small exotherm) resulted in crystallization to apatite and mullite (Fig. 2). However, when this glass was cast from the melt, it produced an opalescent glass, which had partially crystallized to apatite. A transmission electron micrograph of a carbon replica of this glass is shown in Fig. 3.

Droplets in this glass are clearly visible along with hexagonal apatite crystals extracted with the carbon film. The microstructure of this glass is similar to most

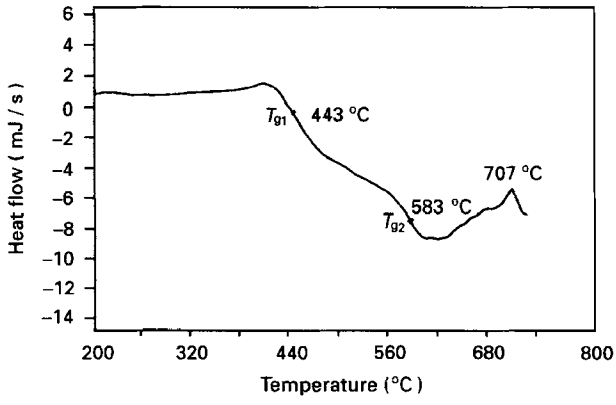

Figure 1 DTA trace showing two glass transition temperatures for the commercial ionomer glass composition.

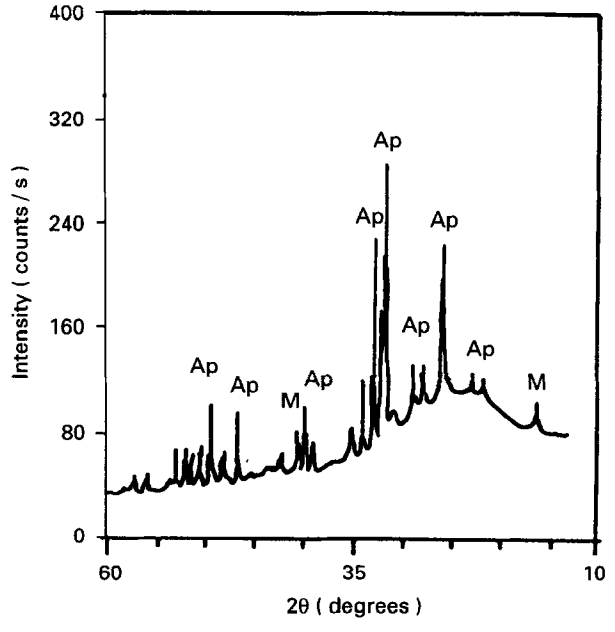

Figure 2 X-ray powder diffraction pattern of a commercial ionomer glass after heat treatment at 930 °C for 20 min: A = apatite, M = mullite.

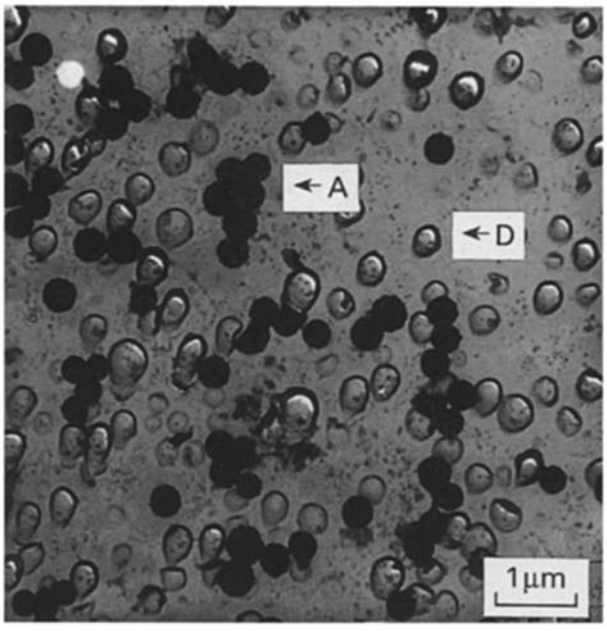

Figure 3 Carbon replica electron micrograph of the cast commercial ionomer glass composition. Note the droplets (D) present as well as the hexagonal apatite (A) crystallites extracted in the replica.

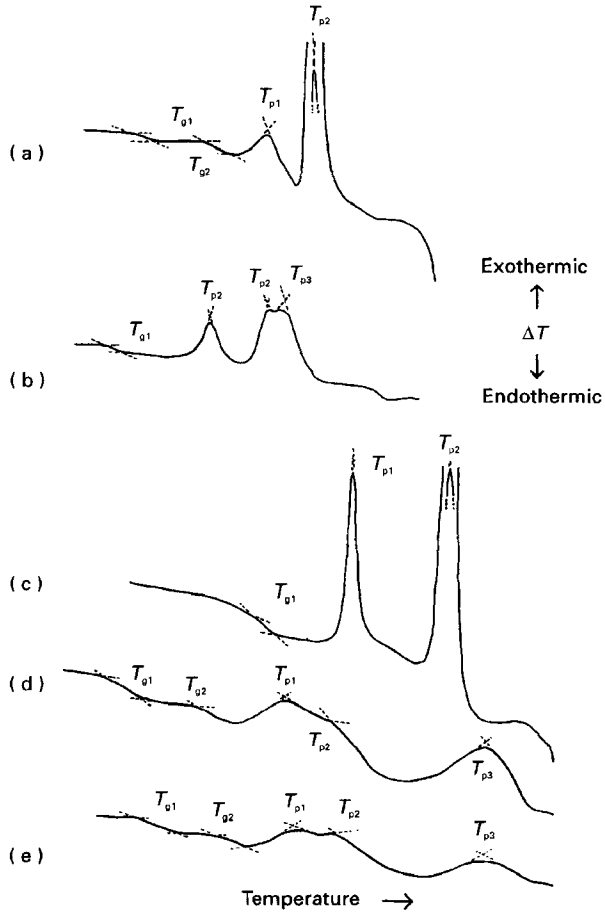

Figure 4 DTA traces for the A series glasses: (a) $X = 0.25$; (b) $X = 0.375$; (c) $X = 0.5$; (d) $X = 0.75$; (e) $X = 1.00$.

other apatite-based glass-ceramics, where the apatite is formed as squat hexagonal crystallites which are contained within a droplet structure, rather than the long needle-shaped crystallites found in natural dentine, enamel and bone. Because of the marked loss of silicon tetrafluoride that occurs when melting this glass composition and the fact that it crystallized during casting, this glass was not considered a practical material for further studies. Subsequent studies concentrated on related glass compositions in which loss of silicon tetrafluoride was suppressed by the presence of basic calcium oxide in the melt.

The first series of glasses investigated were the A series glasses where SiO_2 is replaced successively by P_2O_5. DTA traces for the various glasses are shown in Fig. 4a to e. The DTA traces all show at least two exotherms and in some cases two glass transition temperatures. The glass transition temperatures and peak crystallization temperatures are summarized in Table III. All these glasses were found to crystallize to fluoroapatite and mullite except for the glass with the highest phosphate content, glass A6, which crystallized to apatite and a suspected aluminium phosphate phase. The first crystalline phase formed in all these glasses was always apatite. The inclusion of phosphorous pentoxide in these glasses might have been expected to reduce the glass transition temperature (T_g) and reduce the peak exotherm temperatures (T_p), since the phosphorous–oxygen bond is much weaker than the silicon–oxygen bond. Furthermore, the aluminium ion, Al^{3+} can maintain the local electroneutrality by being closely associated with the phosphorous, P^{5+} ion. This charge balance is achieved by having an AlO_4^- tetrahedra adjacent to a PO_4^+ tetrahedra in the glass network. Thus the inclusion of phosphate in these glasses will release calcium ions from a charge-balancing role and they will then act to disrupt the glass network. Evidence for the close association of AlO_4^- and PO_4^+ species in these glasses is provided by the ease with which glass A6 crystallizes to a suspected aluminium phosphate phase. The introduction of two phosphate species for a silicate species in these glasses will result in an increase in the cross-link density of the glass and this counteracts the latter two effects. The fact that some of these glasses exhibit two glass transitions indicates that these glasses have already undergone APS, or undergo APS during the DTA run.

TABLE III Glass transition temperatures (T_g) and peak crystallization temperatures (T_p) for the A series glasses

Glass code	T_{g_1} (°C)	T_{g_2} (°C)	T_{p_1} (°C)	T_{p_2} (°C)	T_{p_3} (°C)
A1	642		707	876	
A2	631	713	772	834	
A3	631		718	782	801
A4	621		723	814	
A5	662	758	826	878	1037
A6	669	751	818	860	1017

The glass with $X = 0.5$ had a calcium phosphate ratio of 2:1, close to the 1.66:1 found in apatite, and crystallized readily to give a significant volume fraction of fluoroapatite. This glass also crystallized slightly on casting from the melt. It was thought that by reducing the proportion of network modifier present castable homogeneous glasses could be produced that

would crystallize to a large volume fraction of fluoroapatite. Series B glasses were therefore based on this glass, but with a decreasing calcium fluoride content.

Fig. 5 shows the DTA traces for the B series glasses with $Y = 1.00$, 0.5 and 0. There are two sharp exotherms for the glass with the highest fluoride content and only one large broad exotherm for the glass containing no fluoride. The glass transition temperature (T_g) and peak exotherm temperatures T_p are summarized in Table IV. The glass transition temperature reduces as the fluorite content is increased, presumably as a result of the Ca and F atoms disrupting the glass network and replacing bridging oxygens by non-bridging oxygens and non-bridging fluorines. Some glasses show evidence of a possible second glass transition temperature, which may indicate that the glass has undergone amorphous phase separation. The glass with $Y = 1$ and the largest proportion of fluorite shows two sharp crystallization exotherms. As the fluorite content is reduced, the first of these exotherms diminishes until finally there is only one exotherm for the glass with no fluorite.

Selective heat treatments of glasses B1 to B4 followed by subsequent X-ray powder diffraction demonstrated that the first exotherm corresponded to the crystallization of an apatite phase, probably fluoroapatite, while the second exotherm corresponded to the crystallization of mullite and some further apatite. An X-ray powder diffraction pattern for glass B1 after heat treatment at 930 °C for 20 min is shown in Fig. 6. Glass B5 containing no fluorite ($Y = 0$) crystallized to anorthite ($CaAl_2Si_2O_8$) and a very small amount of an apatite phase, which in this case

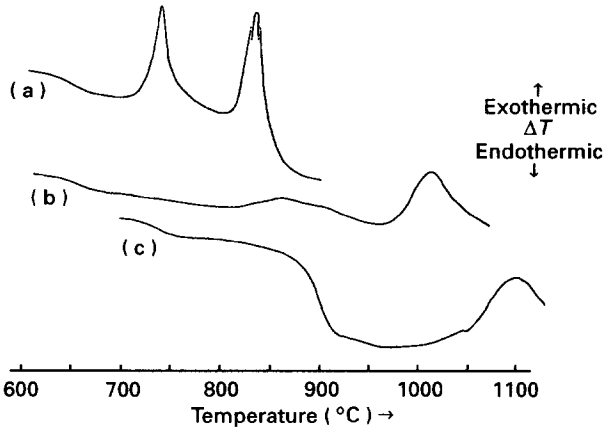

Figure 5 DTA traces for the B series glasses: (a) $Y = 1.00$; (b) $Y = 0.50$; (c) $Y = 0$.

TABLE IV Glass transition temperatures (T_g) and peak crystallization temperatures (T_p) for the B series glasses

Glass code	T_{g_1} (°C)	T_{g_2} (°C)	T_{p_1} (°C)	T_{p_2} (°C)
B1	621	–	723	814
B2	640	–	761	943
B3	668	–	815	987
B4	717	834	–	1079
B5	819	922	–	1095

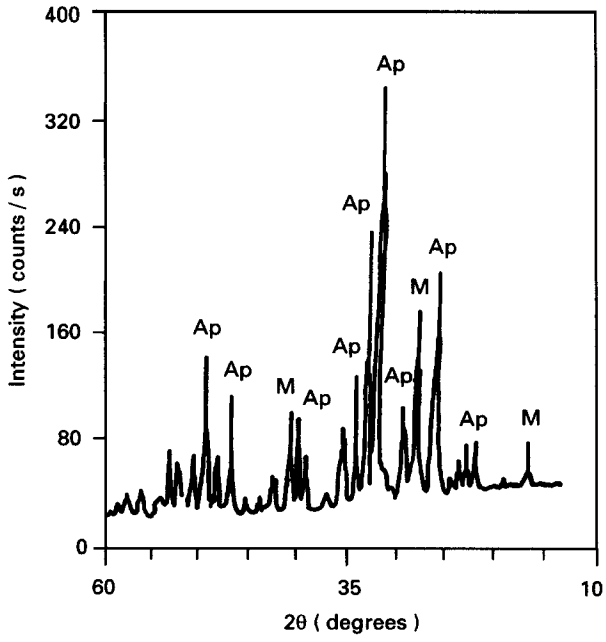

Figure 6 X-ray powder diffraction pattern of glass B1 after heat treatment at 930 °C for 20 min: A = apatite, M = mullite.

TABLE V Effect of particle size on DTA data obtained from the B series glasses

Glass	Particle (μm)	T_{g_1} (°C)	T_{p_1} (°C)	T_{p_2} (°C)
B1	< 45	621	721	818
	> 45	624	724	818
	> 125	625	726	820
B2	< 45	640	761	943
	> 45, < 125	644	755	963
	> 125	644	757	964
B3	< 45	664	816	987
	> 45, < 125	664	876	1015
	> 125	662	923	1037
B4	< 45	717	834	1079
	> 45, < 125	708	856	1096
	> 125	718	–	1086
B5	< 45	819	922	1095
	> 45, < 125	803	955	1148
	> 125	802	971	1169

may well be an oxyapatite, since there is no fluorine and there will be very little water in the glass. The composition with no fluorite is similar to that of bone china, which is also known to crystallize to anorthite.

The mullite and anorthite phases are formed at higher temperatures than the apatite phase because crystallization of these phases will involve breaking and reordering of the strong Si–O and Al–O bonds of the glass network.

One key feature of any practical glass-ceramic is that crystal nucleation should take place readily and rapidly within the bulk of the glass and not take place preferentially at the surface as it does with the A–W glass-ceramics. The contribution of surface nucleation to crystallization is most conveniently studied by carrying out DTA experiments on glass samples with

very different surface areas. The result of such experiments are shown in Table V.

The peak exotherm temperatures (T_p) for glasses B1 and B2 are independent of particle size, indicating that crystallization of both the apatite and mullite crystalline phase proceeds by a bulk nucleation mechanism. In contrast, the glasses with lower fluorite contents exhibit peak exotherm temperatures that move to higher values with increasing particle size; indicating that surface nucleation is now the dominant mechanism of crystal formation.

Attempts to determine optimum nucleation temperatures for all the glasses by the DTA method were unsuccessful as there appeared to be no optimum nucleation temperature. The fact that there was no optimum nucleation temperature and that two of the glasses exhibited bulk crystal nucleation suggested that these glasses underwent crystal nucleation via prior amorphous phase separation. Amorphous phase separation is the dominant crystal nucleation mechanism in commercial glass-ceramics and has been extensively discussed [19, 20]. Crystal nucleation via prior APS generally occurs very rapidly without a prolonged nucleation hold and is therefore attractive commercially, since it leads to short ceramming cycles. Fluorides and phosphates are known to induce amorphous phase separation [21] and it has previously been shown to be the nucleation mechanism in the related phosphate-free glass A1 [22, 23]. All the glasses after appropriate heat treatment were found to undergo amorphous phase separation, prior to crystallization when examined in the SEM (Fig. 7) or using the carbon replica technique and the TEM. Even those glasses (B3, B4 and B5) that did not exhibit any evidence of bulk crystal nucleation were found to have undergone amorphous phase separation. Glass B5 was similar in composition to bone china and some glass-ceramics designed to have similar properties to bone china [24]. These latter glass-ceramics, however, exhibit amorphous phase separation and bulk crystal nucleation. Clearly, amorphous phase separation may, or may not lead to subsequent crystal nucleation. The composition of the droplet and matrix phases formed after amorphous phase separation are probably critical in determining the activation energy barrier for subsequent crystal nucleation. Unfortunately, the size scale of the APS was always well below 1 μm and therefore the composition of the two phases could not be determined using the facilities available.

In glasses B1 and B2, the phase separation occurred just above the glass transition temperature and resulted in an interconnected structure that subsequently broke down to give a droplet structure, in a similar fashion to that observed in the related phosphate-free glass [22, 23]. The interconnected structure may indicate a spinodal decomposition mechanism [25] as opposed to a nucleation mechanism for amorphous phase separation.

A preliminary investigation of the crystal microstrurctural development was undertaken. Holding the fluoride containing glasses for a prolonged period close to the first exotherm corresponding to that of fluoroapatite, resulted in glasses containing long

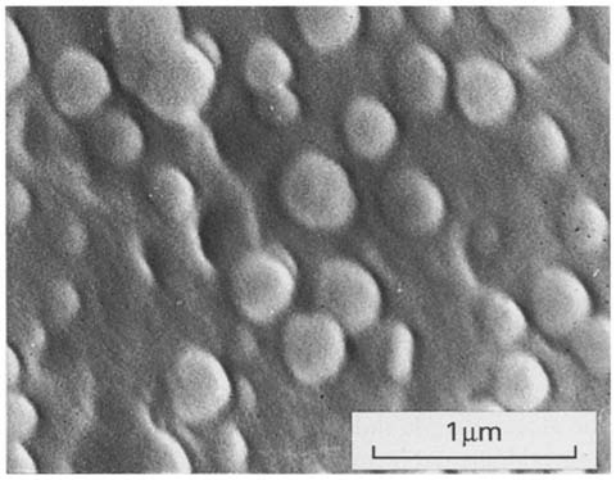

Figure 7 APS observed in glass B5 after heat treatment to 1000 °C.

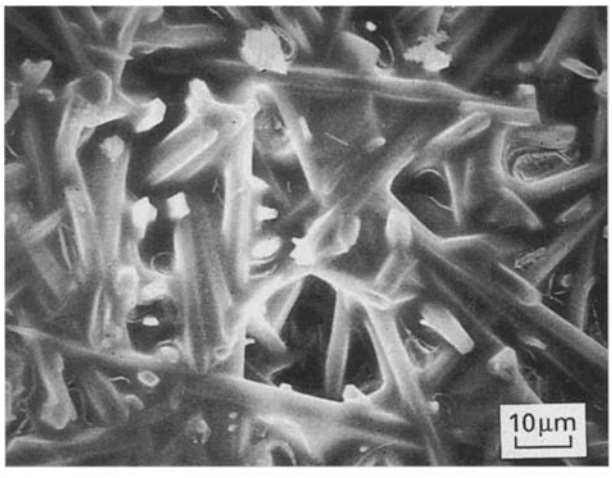

Figure 8 SEM micrograph of glass B3 showing the presence of long fluoroapatite needles after holding for 2 h at the first peak exotherm temperature (816 °C).

needle-like crystals (Fig. 8). These crystals had a length to diameter aspect ratio of the order 50:1, consisted largely of calcium and phosphate and had a hexagonal structure and it was concluded that they consisted of fluoroapatite.

Heat treating to a higher temperature corresponding to the second exotherm and the crystallization of mullite in addition to apatite resulted in a fine microstructure consisting of interlocking apatite and mullite needles (Fig. 9). At higher magnification (Fig. 10) it appears that the mullite crystals have grown around the apatite needles and restricted their growth; as a result they are now much smaller and have been preferentially etched away by the hydrofluoric acid in the preparation of the carbon replicas.

These glass-ceramics differ from all other apatite-based glass-ceramics in that they have a very high fluoride content. In general, apatite-based glass-ceramics contain little or no fluorine. In the cases where small amounts of fluorine are present, it is added at low levels as fluorite and is thought to act as a nucleating agent. In contrast, the apatite–mullite glass-ceramics studied here contain up to 20 mol % fluorite. Most of the published papers on apatite glass-ceramics are not clear as to whether the apatite phase

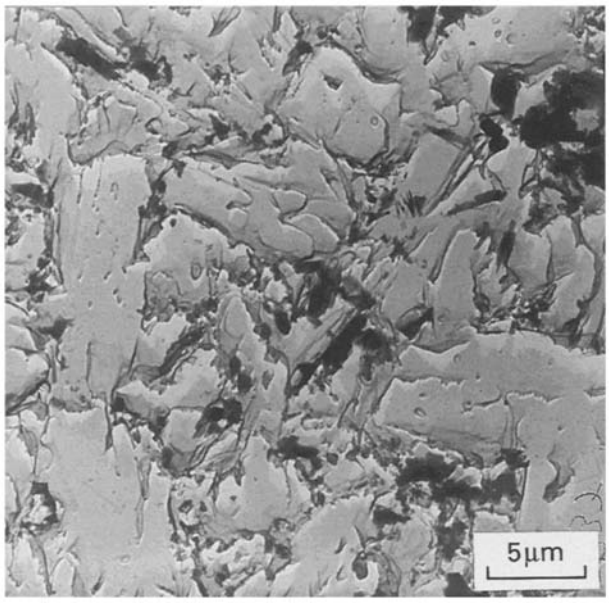

Figure 9 Carbon replica electron micrograph of glass B5 after heat treatment to 1000 °C. Low magnification.

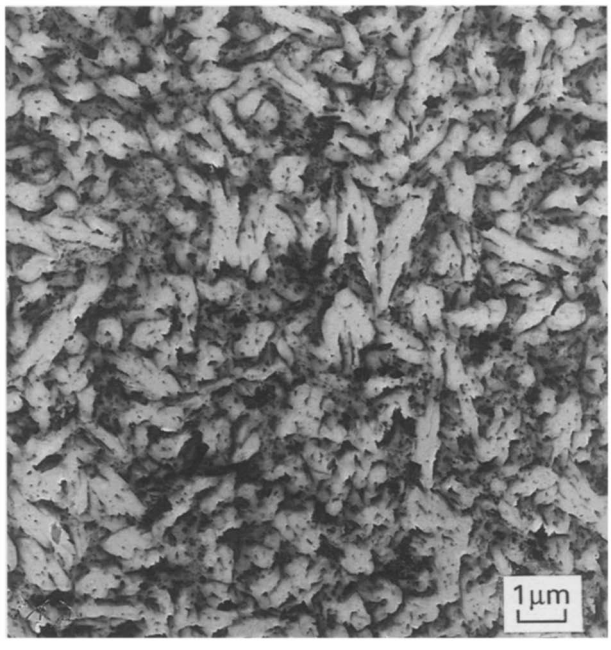

Figure 10 Carbon replica electron micrograph of glass B2 after heat treatment to 1000 °C. High magnification.

formed is fluoroapatite, oxyapatite, hydroxyapatite or a mixed apatite. The lattice parameters for these apatites are so close that it is extremely difficult to distinguish between them by X-ray powder diffraction. However, these various apatites can be distinguished readily by infrared spectroscopy [26] and from infrared spectroscopy studies it is thought that the apatite formed in the present glass-ceramics is fluoroapatite and the apatites formed in most other glass-ceramics are oxyapatite or hydroxyapatite. It is known that fluorine packs exceedingly well into the apatite lattice compared to the oxygen of the hydroxy and oxy forms where, for steric reasons, the oxygen is displaced from the Co axis, which decreases the symmetry and stability of the crystal. Fluorides induce a woven bone pereosteum *in vivo* at high concentrations and result in larger, longer, more clearly defined apatite crystals. The better packing of fluorine within the apatite crystal may therefore explain the ease with which fluorapatite undergoes bulk crystals nucleation and the formation of long needle-shaped fluoroapatite crystals. In contrast, in all other apatite glass-ceramics, the apatite does not form needle-shaped crystals and does not generally undergo such ready bulk crystal nucleation, which is a pre-requisite for a successful glass-ceramic.

5. Conclusions

Fluoro-alumino-silicate glasses of similar composition to existing ionomer glasses used to produce polyalkenoate dental cements, but containing a basic oxide to prevent fluorine loss from the melt, exhibit a low liquidus temperature and can be readily cast. Compositions with high fluoride content undergo bulk crystal nucleation, with appropriate heat treatment, to fluoroapatite and mullite. Both crystal phases exhibit a needle-like crystal morphology with the fluoroapatite forming crystals with a particular high length to diameter aspect ratio, similar to that found *in vivo*.

Further work is required to study the influence of thermal treatment on microstructural development in these unique glass-ceramics and subsequently to study the relationship between microstructure and strength. The biocompatibility of any glass-ceramics developed as bone substitutes would also need to be investigated.

References

1. T. KOKUBO, M. SHIGEMATSU, Y. NAGASHIMA, T. TASHIRO, T. NAKAURA, T. YAMAMURO and H. HIGASHI *Bull. Inst. Chem. Red Kyoto Univ.* **30** (1982) 260.
2. G.J.H. BEALL, M.R. MONTIERTH and P. SMITH *Barbeithare Glaskeramik Umshace* **42** (1972) 468.
3. D.G. GROSSMAN, US Patent 3839055 (1974).
4. W. VOGEL, W. HOLAND, K. NAUMANN and J. GUMMEL, *J. Non-Cryst. Solids* **80** (1986) 34.
5. H. BROMER, K. DEUTSCHER, B. BLENKE, E. PFEIL and V. STRUNZ, *Sci. Ceram.* **9** (1977) 219.
6. T. KOKUBO, S. ITO, S. SAKKO and T. YAMAMURO, *J. Mater. Sci.* **21** (1986) 536.
7. W.T. MACCULLOCH, *Brit. Dent. J.* **124** (1968) 361.
8. S. HOBO and T. IWATA *Quintessence Int.* **16** (1985) 207.
9. S. HOBO and T. IWATA *ibid.* **7** (1985) 451.
10. P. MARQUIS, "Dental Ceramics" *Met. Mater.* March (1989) 145.
11. P.J. ADAIR and D.G. GROSSMAN, *Int. J. Periodont, Res. Dent* **4** (1984) 683.
12. R.G. HILL, M. PATEL and D.J. WOOD, in: Bioceramics", Vol. 4, edited by W. Bonfield, G.W. Hastings and K.E. Tanner (Butterworth Heinemann, London, 1991).
13. R.T. TURNER, R. FRANCIS, D. BROWN, J. GARAND, K.S. HANNON and N.H. BELL, *J. Bone Mater. Res.* **4** (1984) 477.
14. M. OKAZAK and M. SATO, *Biomaterials* **11** (1990) 573–578.
15. M. OKAZAK, T. AOBA, T. DIO, J. TAKAHASH and Y. MORIWAKI, *J. Dent. Res.* **60** (1981) 845.
16. M. OKAZAK, J. TAKAHASHI, H. KIMURA and T. AOBA, *J. Biomed Mater. Res.* **16** (1982) 851.
17. D. WOOD and R. HILL, *Clin. Mater.* **7** (1991) 301.
18. E.A. WASSON and J.W. NICHOLSON, *Brit Polym. J.* **23** (1990) 179.

19. P.F. JAMES, in "Advances in ceramics 4 Nucleation and crystallisation in glasses," edited by J.H. Simmons, D.R. Uhlmann and G.H. Beall (American Ceramic Society, Ohio, 1982).
20. P.F. JAMES, in "Glasses and glass-ceramics", edited by M.H. Lewis (Chapman and Hall, London, 1989).
21. P.W. McMILLAN, "Glass-ceramics", 2nd End (Academic Press, London, 1979).
22. R.G. HILL, C. GOAT and D.J. WOOD, *J. Amer. Ceram. Soc.* **75** (1992).
23. D. WOOD and R. HILL, *Biomaterials* **12** (1991) 164
24. British Patent Specification 869, 315 (1961)
25. J.W. CAHN, *Acta Metall.* **9** (1961) 795.
26. J. COOPER, *Interceram.* **41** (1989) 271.

Received 23 September 1993
and accepted 17 May 1994